JACS
JOURNAL OF THE AMERICAN CHEMICAL SOCIETY
Communication
pubs.acs.org/JACS

Very Low Band Gap Thiadiazoloquinoxaline Donor–Acceptor Polymers as Multi-tool Conjugated Polymers

Timothy T. Steckler,[†,‡] Patrik Henriksson,[†,‡] Sonya Mollinger,[§,‡] Angelica Lundin,[†] Alberto Salleo,*[,§] and Mats R. Andersson*[,†]

[†]Department of Chemical and Biological Engineering, Chalmers University of Technology, SE-412 96 Gothenburg, Sweden
[§]Department of Materials Science, Stanford University, Stanford, California 94305-4034, United States

Supporting Information

ABSTRACT: Here we report on the synthesis of two novel very low band gap (VLG) donor–acceptor polymers ($E_g \leq 1$ eV) and an oligomer based on the thiadiazoloquinoxaline acceptor. Both polymers demonstrate decent ambipolar mobilities, with **P1** showing the best performance of $\sim 10^{-2}$ cm^2 V^{-1} s^{-1} for p- and n-type operation. These polymers are among the lowest band gap polymers ($\lesssim$0.7 eV) reported, with a neutral λ_{max} = 1476 nm (**P2**), which is the farthest red-shifted λ_{max} reported to date for a soluble processable polymer. Very little has been done to characterize the electrochromic aspects of VLG polymers; interestingly, these polymers actually show a bleaching of their neutral absorptions in the near-infrared region and have an electrochromic contrast up to 30% at a switching speed of 3 s.

Soluble donor–acceptor (DA) polymers offer the advantages of being the "Swiss Army knife" of conjugated polymers, with numerous applications in organic electronics such as organic solar cells (OSCs),[1−3] organic field-effect transistors (OFETs),[4−7] light-emitting diodes (LEDs),[8−10] and electrochromics.[11−13] Sometimes the same polymer performs quite well in more than one application, such as a diketopyrrolopyrrole-based polymer in OFETs and OSCs.[14] In other cases, it takes only a slight modification of the main DA core, as in isoindigo polymers, to tailor the properties for different applications such as OSCs and OFETs.[6,15] By choosing the proper donor (π-electron-rich) and acceptor (π-electron-deficient) units, one can tailor the properties of the resultant polymer for various applications in organic electronics.[16−19] Recent work has shown that very low band gap (VLG, ≤1 eV) DA polymers using the benzobisthiadiazole (BBT) acceptor, have proven to yield ambipolar and high-mobility polymers (mobilities as high as 1 cm^2 V^{-1} s^{-1}).[4,7,20] This behavior can partially be attributed to the fact that these polymers have both high electron affinities and low ionization potentials, which can aid the injection of both holes and electrons at moderate potentials for ambipolar charge transport.

While much research on VLG DA polymers has been focused on OFETs and OSCs,[4,21,22] very little has been done to characterize the electrochromism aspect of these polymers.[23] Since DA polymers have access to multiple redox states in a small potential window, these materials can be potentially useful in electrochromic devices, supercapacitors, batteries, and sensors.[24] The ability to tune the color by structural alterations of the polymer, solution processability, low oxidation potential and thin film flexibility are all advantages of organic polymers over inorganic compounds.[13,25,26] For these VLG DA polymers that switch in the near-infrared (NIR) region, some suggested applications have been as battlefield camouflage countermeasures against night vision equipment and for spacecraft thermal control, taking advantage of the polymers' light weight.[27]

In the present work we focus on the characterization of two VLG DA polymers incorporating the thiadiazoloquinoxaline (TQ) acceptor. Some of the advantages of this acceptor compared to the slightly stronger BBT acceptor are that the TQ acceptor can be functionalized with various aryl or alkyl groups, thus improving the solubility immensely. Having improved solubility in the acceptor will not only allow for higher molecular weight polymers, but it will also allow for DA polymers to be made with just a single thiophene donor. This cannot be said so far for past TQ- or BBT-based polymers, which normally have the acceptor flanked by two or more donor units substituted for improved solubility or a fused donor unit with inherent solubility.[4,7,21−23,28,29] Previous TQ-based polymers have proven useful as the active materials in OSCs and OFETs.[22,23,28]

Here we report the synthesis and properties of an oligomer and two DA polymers (Figure 1) that incorporate just one single thiophene donor unit combined with one of two TQ acceptors that vary only in the aryl substitution position (para, **O1** and **P1**, vs meta, **P2**) of the octyldodecyloxy side chain. To gain more insight into the optical and electronic properties of these polymers, quantum-chemical simulations were performed and compared to experimental results for **O1**, **P1**, and **P2**. As these polymers are inherently interesting due to their high electron affinities and low ionization potentials, investigation into their performance as active materials in OFETs and electrochromic devices was performed.

The synthesis of **O1**, **P1**, and **P2** is described in the Supporting Information (Schemes S1–S3). Stille polymerization of TQ acceptors **4** and **5** with 2,5-bistrimethylstannylthiophene yielded polymers **P1** and **P2** as dark brown solids in high yields (≥88%). Further synthetic details and purification procedures are given in the Supporting Information. Both

Received: October 14, 2013
Published: December 18, 2013

ACS Publications © 2013 American Chemical Society

dx.doi.org/10.1021/ja410527n | J. Am. Chem. Soc. 2014, 136, 1190–1193

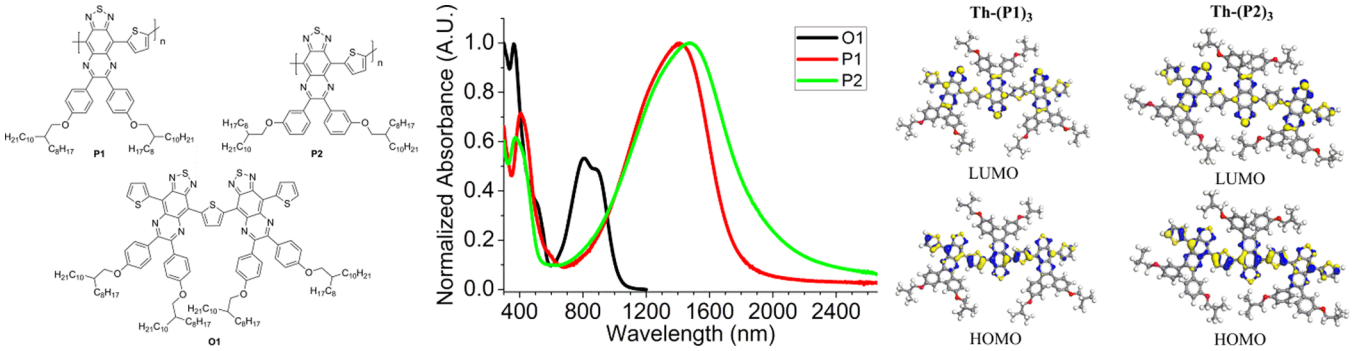

Figure 1. (Left) Chemical structures of the polymers and oligomer discussed in the present study. (Middle) UV−vis−NIR absorption spectra of thin films of **O1**, **P1**, and **P2**. (Right) Visualization of the HOMO/LUMO levels for oligomers **Th-(P1)**$_3$ and **Th-(P2)**$_3$.

polymers were of high molecular weight (**P1**, M_n = 274 kDa, PDI = 6.3; **P2**, M_n = 45 kDa, PDI = 6.3) and thermally stable, with 1% weight loss occurring above 400 °C under a nitrogen atmosphere.

Geometric structures and optical and electronic properties of all polymers were calculated on the basis of density functional theory (DFT) calculations on thiophene end-capped trimers (Tables S2 and S3, Figures 1, S3, and S4) based on the repeating units in **P1** and **P2**, **Th-(P1)**$_3$ and **Th-(P2)**$_3$, using a GGA functional PW91 with a double numerical plus d-functions on heavy elements and p-functions on hydrogen (DNP, basis file 4.4), and those structures and properties are used throughout this study.[30] Both **Th-(P1)**$_3$ and **Th-(P2)**$_3$ oligomers are predicted to have strong absorptions in the NIR, peaking at 1395 and 1432 nm, respectively (Figures S3 and S4). These λ_{max} are associated with HOMO−LUMO+1 transitions, whereas the furthest red-shifted absorptions, which are of smaller intensity, are at 1528 and 1523 nm for **Th-(P1)**$_3$ and **Th-(P2)**$_3$. These lowest energy absorptions are associated with HOMO−LUMO transitions. In both models, the HOMO wave functions are delocalized along the polymer backbone while the LUMO wave functions are mainly localized on the TQ acceptors (Figure 1). This indicates these polymers should have quite a low band gap with their absorptions in the NIR having a high degree of charge transfer. The predicted band gaps for these oligomers (Table S3) are 0.93 eV for **Th-(P1)**$_3$ and 0.94 eV for **Th-(P2)**$_3$, which also indicate these polymers should have quite a low band gap.

Optical absorption spectra of thin films (solution) of **O1**, **P1**, and **P2** can be seen in Figure 1 (Figure S1), and their associated properties are summarized in Table S1. In the solid state, **O1**, **P1**, and **P2** have the typical two-band absorption profiles seen in many DA polymers, with λ_{max} = 809 (875 nm, sh), 1410, and 1476 nm, respectively.[16] While the λ_{max} values are red-shifted 34, 57, and 55 nm respectively for **O1**, **P1**, and **P2** when going from solution to film, the onset of absorption for these materials is more significantly red-shifted. The fact that the λ_{max} values for **P1** and **P2** are beyond 1400 nm is quite remarkable considering the TQ-based acceptor is not as strong as the BBT-based acceptor, yet **P2** has its λ_{max} for a neutral conjugated polymer located farthest into the NIR to date (1476 nm). To make sure these neutral absorptions are not doped states, thin films were spin-coated onto glass slides and absorption spectra were measured before and after dipping the film into a 5% hydrazine/acetonitrile solution (Figure S1), and showed minimal changes in absorption profile. Optical band gaps for **O1**, **P1**, and **P2**, determined by the onset of absorption using a tangent line from the peak absorption to the baseline, were determined to be 1.22, 0.71, and 0.64 eV, respectively. The low band gaps for these polymers, especially **P2**, are among the lowest reported to date, and are in the class of the reported BBT-based polymers.[4,7,23,29,31] The general trends of the theoretical absorption spectra (Figures S3 and S4) based on the oligomers of **P1** and **P2** match up accordingly with the actual absorption spectra of the polymers, with both polymers having a much more intense absorption in the NIR region compared to the UV−vis region. These intense absorptions in the NIR correspond to HOMO−LUMO or HOMO−LUMO+1 transitions, which show heavily localized LUMO wave functions on the TQ acceptors (Figures 1, S3, and S4). This is in good agreement with most calculations on low band gap DA polymer systems and shows a large degree of charge transfer.[4,6,23,32]

The electrochemical properties of **P1** and **P2** were investigated using square-wave voltammetry (Figure S2) on polymer thin films and are summarized in Table S2. HOMO/LUMO levels were extrapolated from the onset potentials for oxidation and reduction. **P1** has a HOMO level of −5.17 eV, a LUMO of −4.21 eV, and an electronic band gap of 0.96 eV. It is important to note that **P1** has the 2-octyldodecyloxy side chain in the para position, which increases the electron density on the acceptor, thus making it a slightly weaker acceptor, compared to **P2**, which has the side chain in the meta position. Likewise, **P2** has a HOMO level of −5.21 eV, a LUMO of −4.29 eV, and a slightly smaller electronic band gap of 0.92 eV. While the HOMO/LUMO levels predicted by DFT calculations in Table S3 are significantly higher (∼0.6−0.7 eV) than the actual values, the band gaps are in excellent agreement with the predicted values of 0.93 and 0.94 eV for **P1** and **P2**, respectively. The electronic band gaps determined here are somewhat larger than their optical band gaps, as has been observed for many polymers.[4] The trend is in good agreement with the optical band gaps based on the different acceptor strengths of these two polymers as a result of the side-chain positioning. While the difference in absorption of these two polymers could be attributed to the solid-state packing, it is most likely due to the acceptor strength based on the solution UV−vis−NIR absorption measurements where aggregation should be diminished (Figure S1) and the fact that they have very similar 2-D grazing incidence X-ray diffraction patterns (discussed later), suggesting similarly ordered systems.

Since **P1** and **P2** have such strong absorption in the NIR region and switch in a small potential window, they are good candidates for potential applications in electrochromic devices

dx.doi.org/10.1021/ja410527n | J. Am. Chem. Soc. 2014, 136, 1190−1193

that modulate NIR absorption. To investigate the polymers in more detail, spectroelectrochemistry was performed on spray-cast thin films of **P2** (Figure 2) and **P1** (Figure S5) on ITO-

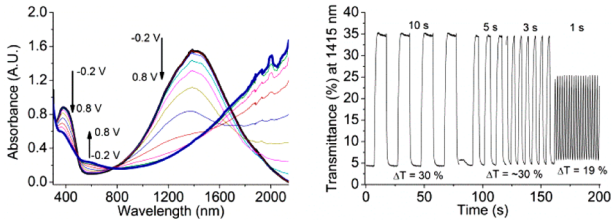

Figure 2. Oxidative spectroelectrochemistry of **P2** (left) spray-coated on an ITO-coated glass slide working electrode switching between −0.2 and 0.8 V in 0.1 V increments. Square-wave potential step absorptometry of **P2** (right) switching between −0.2 and 0.8 V measured at the low-energy peak, 1415 nm, at various residence times.

coated glass working electrodes. The polymers were cycled ∼7−8 times until a stable spectra was reached in 0.1 M solution of tetrabutyl ammonium hexafluorophosphate (Bu_4NPF_6) in anhydrous acetonitrile before analysis. Both polymers have two peak absorptions, one on the border of the UV−vis region (∼378 nm **P2**, ∼401 nm **P1**) and the other in the NIR region (∼1415 nm **P2**, ∼1369 nm **P1**), resulting in a light yellow/brown (**P2**) or light brown (**P1**) thin film. Upon application of incremental oxidative potentials, both polymers undergo similar changes, where the two neutral absorptions start to bleach while the charge carrier bands beyond 2000 nm start to form. Most notably is the bleaching of the NIR neutral absorption in both polymers. Spectroelectrochemistry performed on some VLG BBT-based polymers shows that the charge carrier band formation overlaps directly with the neutral NIR absorption, thus there is no bleaching in the NIR region,[23,31] whereas in these polymers, we observe an actual bleaching of the NIR neutral absorption while the charge carrier bands form farther out into the NIR.

Given that spectroelectrochemistry demonstrated that both of these polymers actually bleach their neutral absorptions, electrochromic devices were constructed and square-wave potential step absorptometry was performed, where the transmittance was monitored at 1415 nm for **P2** (Figure 2) and 1350 nm for **P1** (Figure S5). Tandem chronocoulometry was also performed in the case of **P1** (a limited amount of **P2** precluded it from this study) in order to determine the coloration efficiency (Table S4).[33] **P2** showed the highest electrochromic contrast (EC) ($\Delta\%T$) of 30% at switching times as fast as 3 s with an average switching time for a 95% contrast switch of 1.93 s. At 1 s switching times, the EC drops to 19%. Meanwhile, **P1** had a maximum EC of 26% while maintaining its contrast down to 1 s switching times (Figure S5). The average switching time for **P1** is 0.48 s with a coloration efficiency 1253 cm^2/C (Table S4). While the EC of these polymers are modest, the stability of these devices are quite good with **P1** retaining or slightly increasing (27%) its EC down to 3 s switches, with a minimal decrease in EC to 25.4% after 2000 switches. The average switching time for **P1** increased to 0.84 s with a slight decrease in CE to 1043 cm^2/C. This is the first demonstration of the bleaching of a neutral polymer NIR absorption at such a long wavelength.

The small difference in the HOMO/LUMO levels of polymers **P1** and **P2** suggests that they may be capable of ambipolar charge transport and could perform well in OFETs. Bottom gate top contact (BGTC) devices were constructed on heavily doped silicon wafers. Thermally grown 200 nm SiO_2 acted as a gate dielectric, and the substrate was treated with octadecyltrichlorosilane (OTS). Polymer films were then deposited via spin-coating from chloroform solutions followed by thermal evaporation of gold contacts.

Representative transfer and output characteristics from OTS-treated BGTC devices using **P1** (**P2**) can be seen in Figure 3

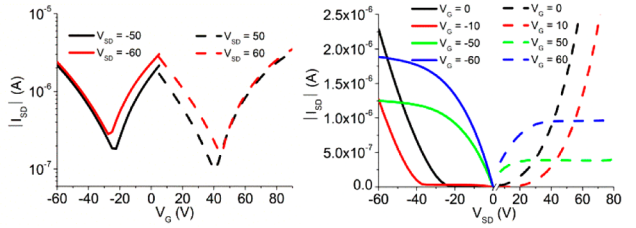

Figure 3. Transfer characteristics of OTS-treated BGTC OFETs using **P1** as the active layer (left). Output characteristics for OTS-treated BGTC OFETs using **P1** as the active layer (right).

(Figure S8) and are summarized in Table S5. Both polymers showed ambipolar behavior. Devices using **P1** as the active layer resulted in average mobilities of $3.0 \times 10^{-2} \pm 6 \times 10^{-3}$ $cm^2\ V^{-1}\ s^{-1}$ for p-type and $1.4 \times 10^{-2} \pm 1 \times 10^{-2}$ $cm^2\ V^{-1}\ s^{-1}$ for n-type operation, while **P2** had average mobilities of $1.1 \times 10^{-3} \pm 8 \times 10^{-4}$ $cm^2\ V^{-1}\ s^{-1}$ for p-type and $2.0 \times 10^{-2} \pm 1 \times 10^{-2}$ $cm^2\ V^{-1}\ s^{-1}$ for n-type operation. To investigate if device architecture influenced the mobility, top gate bottom contact (TGBC) devices (Figures S9 and S10) were also investigated. While TGBC devices performed quite similarly to BGTC devices (Figures S6 and S7) on untreated substrates, OTS-treated BGTC devices resulted in the best performance for both polymers. The comparison of their performance characteristics can be seen in Table S5.

Generally, **P1** performed better than **P2** as an ambipolar polymer in all OFET architectures investigated in this study. While the polymer structures do vary in terms of meta (**P2**) verses para (**P1**) positioning of the side-chain on the phenylenes, the HOMO/LUMO levels for both polymers are quite similar, with **P2** having slightly deeper HOMO/LUMO levels by 40 and 80 meV respectively. However, the major difference between the two polymers is molecular weight, with **P1** (274 kDa) being significantly higher than **P2** (45 kDa). This has been shown in other studies to be quite important in terms of performance.[4]

In order to understand the difference between these two polymers further, investigation into the ordering of these systems were performed using 2D grazing incidence X-ray scattering (Figure S11). Both polymers show a broad halo of diffraction, indicating disorder in the films. The intensity is likely due to π-stacking diffraction, and for both **P1** and **P2** the distance associated with the q_{xy} diffraction is at 4.46 Å. The intensity is much stronger in the q_z direction, indicating a primarily face-on configuration in the bulk. The main difference between the two polymers is the degree to which diffraction is broadened in the q_z direction, with the **P1** intensity shifted to peak at 3.76 Å and **P2** to 3.70 Å. The intensity magnitudes are very similar for both polymers. Even though the polymers have different side-chain positioning, their ordered regions seem to be similar. DSC of both polymers showed no thermal transitions.

dx.doi.org/10.1021/ja410527n | J. Am. Chem. Soc. 2014, 136, 1190−1193

In conclusion, we have synthesized two new, soluble, VLG TQ-based DA polymers which have their λ_{max} located farthest into the NIR at 1410 (**P1**) and 1476 nm (**P2**). Interestingly, the neutral long-wavelength absorptions of both polymers bleach upon incremental oxidation, and moderate EC contrasts of 30% (**P2**) and 25% (**P1**) were obtained. These polymers could prove useful for organic photodetectors or applications where modulation of NIR radiation is necessary, such as thermal emissivity applications. The use of **P1** or **P2** as the active materials in OTS-treated BGTC OFETs resulted in ambipolar transistors with **P1** having the best ambipolar mobilities of $3.0 \times 10^{-2} \pm 6 \times 10^{-3}$ cm^2 V^{-1} s^{-1} for p-type and $1.4 \times 10^{-2} \pm 1 \times 10^{-2}$ cm^2 V^{-1} s^{-1} for n-type operation. With many potential applications, investigation into further structural modifications of these polymers is ongoing for increased performance in all applications.

■ ASSOCIATED CONTENT

Supporting Information

Experimental details, results, and synthetic preparation. This material is available free of charge via the Internet at http://pubs.acs.org.

■ AUTHOR INFORMATION

Corresponding Authors

asalleo@stanford.edu

mats.andersson@chalmers.se

Author Contributions

‡T.T.S., P.H., and S.M. contributed equally.

Notes

The authors declare no competing financial interest.

■ ACKNOWLEDGMENTS

We thank the European Community's Seventh Framework Program (FP7/2007-2013) under grant agreement no. 212311 of the ONE-P project, The Swedish Energy Agency, and the Chalmers Area of Advance, Materials Science for funding. We also thank Anders Mårtensson for GPC measurements and Stefan Hellström for additional electrochemical measurements. S.M.acknowledges financial support in the form of a Stanford Graduate Fellowship.

■ REFERENCES

(1) Kim, Y.; Yeom, H. R.; Kim, J. Y.; Yang, C. *Energy Environ. Sci.* **2013**, *6*, 1909.

(2) Dou, L.; You, J.; Yang, J.; Chen, C.-C.; He, Y.; Murase, S.; Moriarty, T.; Emery, K.; Li, G.; Yang, Y. *Nat. Photon.* **2012**, *6*, 180.

(3) Amb, C. M.; Chen, S.; Graham, K. R.; Subbiah, J.; Small, C. E.; So, F.; Reynolds, J. R. *J. Am. Chem. Soc.* **2011**, *133*, 10062.

(4) Yuen, J. D.; Wudl, F. *Energy Environ. Sci.* **2013**, *6*, 392.

(5) Shahid, M.; McCarthy-Ward, T.; Labram, J.; Rossbauer, S.; Domingo, E. B.; Watkins, S. E.; Stingelin, N.; Anthopoulos, T. D.; Heeney, M. *Chem. Sci.* **2012**, *3*, 181.

(6) Lei, T.; Dou, J.-H.; Ma, Z.-J.; Yao, C.-H.; Liu, C.-J.; Wang, J.-Y.; Pei, J. *J. Am. Chem. Soc.* **2012**, *134*, 20025.

(7) Fan, J.; Yuen, J. D.; Wang, M.; Seifter, J.; Seo, J.-H.; Mohebbi, A. R.; Zakhidov, D.; Heeger, A.; Wudl, F. *Adv. Mater.* **2012**, *24*, 2186.

(8) Sun, M.; Jiang, X.; Liu, W.; Zhu, T.; Huang, F.; Cao, Y. *Synth. Met.* **2012**, *162*, 1406.

(9) Li, P.; Fenwick, O.; Yilmaz, S.; Breusov, D.; Caruana, D. J.; Allard, S.; Scherf, U.; Cacialli, F. *Chem. Commun.* **2011**, *47*, 8820.

(10) Chen, L.; Zhang, B.; Cheng, Y.; Xie, Z.; Wang, L.; Jing, X.; Wang, F. *Adv. Funct. Mater.* **2010**, *20*, 3143.

(11) Amb, C. M.; Dyer, A. L.; Reynolds, J. R. *Chem. Mater.* **2011**, *23*, 397.

(12) Amb, C. M.; Beaujuge, P. M.; Reynolds, J. R. *Adv. Mater.* **2010**, *22*, 724.

(13) Beaujuge, P. M.; Ellinger, S.; Reynolds, J. R. *Nat. Mater.* **2008**, *7*, 795.

(14) Bronstein, H.; Chen, Z.; Ashraf, R. S.; Zhang, W.; Du, J.; Durrant, J. R.; Shakya Tuladhar, P.; Song, K.; Watkins, S. E.; Geerts, Y.; Wienk, M. M.; Janssen, R. A. J.; Anthopoulos, T.; Sirringhaus, H.; Heeney, M.; McCulloch, I. *J. Am. Chem. Soc.* **2011**, *133*, 3272.

(15) Wang, E.; Ma, Z.; Zhang, Z.; Vandewal, K.; Henriksson, P.; Inganäs, O.; Zhang, F.; Andersson, M. R. *J. Am. Chem. Soc.* **2011**, *133*, 14244.

(16) Beaujuge, P. M.; Amb, C. M.; Reynolds, J. R. *Acc. Chem. Res.* **2010**, *43*, 1396.

(17) Roncali, J. *Macromol. Rapid Commun.* **2007**, *28*, 1761.

(18) van Mullekom, H. A. M.; Vekemans, J. A. J. M.; Havinga, E. E.; Meijer, E. W. *Mater. Sci. Eng., R* **2001**, *32*, 1.

(19) Duan, C.; Huang, F.; Cao, Y. *J. Mater. Chem.* **2012**, *22*, 10416.

(20) Kai-Fang, C.; Chu-Chen, C.; Chia-Hung, L.; Wen-Chang, C. *J. Polym. Sci., Part A: Polym. Chem.* **2008**, *46*, 6305.

(21) Dexter Tam, T. L.; Salim, T.; Li, H.; Zhou, F.; Mhaisalkar, S. G.; Su, H.; Lam, Y. M.; Grimsdale, A. C. *J. Mater. Chem.* **2012**, *22*, 18528.

(22) Zoombelt, A. P.; Fonrodona, M.; Wienk, M. M.; Sieval, A. B.; Hummelen, J. C.; Janssen, R. A. J. *Org. Lett.* **2009**, *11*, 903.

(23) Zhang, X.; Steckler, T. T.; Dasari, R. R.; Ohira, S.; Potscavage, W. J., Jr; Tiwari, S. P.; Coppee, S.; Ellinger, S.; Barlow, S.; Bredas, J.-L.; Kippelen, B.; Reynolds, J. R.; Marder, S. R. *J. Mater. Chem.* **2010**, *20*, 123.

(24) Skotheim, T. A., Reynolds, J. R., Eds. *Handbook of Conducting Polymers, Third ed.: Conjugated Polymers, Theory, Synthesis, Properties, and Characterization*; CRC Press LLC: Boca Raton, FL, 2007.

(25) Argun, A. A.; Aubert, P.-H.; Thompson, B. C.; Schwendeman, I.; Gaupp, C. L.; Hwang, J.; Pinto, N. J.; Tanner, D. B.; MacDiarmid, A. G.; Reynolds, J. R. *Chem. Mater.* **2004**, *16*, 4401.

(26) Sonmez, G.; Wudl, F. *J. Mater. Chem.* **2005**, *15*, 20.

(27) Chandrasekhar, P.; Zay, B. J.; Birur, G. C.; Rawal, S.; Pierson, E. A.; Kauder, L.; Swanson, T. *Adv. Funct. Mater.* **2002**, *12*, 95.

(28) Dallos, T.; Beckmann, D.; Brunklaus, G.; Baumgarten, M. *J. Am. Chem. Soc.* **2011**, *133*, 13898.

(29) Yuen, J. D.; Kumar, R.; Zakhidov, D.; Seifter, J.; Lim, B.; Heeger, A. J.; Wudl, F. *Adv. Mater.* **2011**, *23*, 3780.

(30) Perdew, J. P.; Wang, Y. *Phys. Rev. B* **1992**, *45*, 13244.

(31) Steckler, T. T.; Zhang, X.; Hwang, J.; Honeyager, R.; Ohira, S.; Zhang, X.-H.; Grant, A.; Ellinger, S.; Odom, S. A.; Sweat, D.; Tanner, D. B.; Rinzler, A. G.; Barlow, S.; Brédas, J. L.; Kippelen, B.; Marder, S. R.; Reynolds, J. R. *J. Am. Chem. Soc.* **2009**, *131*, 2824.

(32) Lei, T.; Cao, Y.; Zhou, X.; Peng, Y.; Bian, J.; Pei, J. *Chem. Mater.* **2012**, *24*, 1762.

(33) Gaupp, C. L.; Welsh, D. M.; Rauh, R. D.; Reynolds, J. R. *Chem. Mater.* **2002**, *14*, 3964.